

# ATLAS: Assistive Tool for seLf-Aligning Schlieren

Nicholas A. Mejia\* and Bryan E. Schmidt†  
Case Western Reserve University, Cleveland, OH 44106, USA

An assistive tool called ATLAS (Assistive Tool for seLf-Aligning Schlieren) has been produced which takes various “must-haves” for a self-aligning focusing schlieren system as inputs and assists in the placement, sizing, and design choice of the necessary optical components. A step-by-step walkthrough of building a self-aligning focusing schlieren system of the kind in the FPI lab at CWRU has been presented for first-time users of this type of system, along with descriptions of using ATLAS to construct such a system. A list of components of the FPI-CWRU system is provided in the Appendix, along with various issues experienced by the team and their associated solutions in tabulated form. The paper contains a URL to the FPI research website with a downloadable Microsoft Excel Spreadsheet containing ATLAS.

## Nomenclature

$\alpha$	=	Rochon prism interface angle [deg]
$\beta$	=	Rochon prism exit beam or splitting angle [deg]
$C_{\text{source/cutoff}}$	=	source/cutoff grid spatial frequency [lp/mm]
CD	=	condenser/diffuser lens
$d_{M-N}$	=	distance from component M to component N [mm]
$\delta_{\text{cutoff}}$	=	cutoff grid translation adjustment [mm]
$f_M$	=	focal length of component M [mm]
$h_{\text{RP}}$	=	Rochon prism height [mm]
LP	=	linear polarizer
LCP	=	left circularly polarized
LHP	=	linear horizontally polarized
LVP	=	linear vertically polarized
RBG	=	retroreflective background
RL	=	relay lens
RCP	=	right circularly polarized
$TW^M$	=	The $M^{\text{th}}$ test section window
$t_{\text{RP}}$	=	Rochon prism thickness [mm]
QWF	=	quarter-wave film
QWP	=	quarter-wave plate
$w_{\text{RP}}$	=	Rochon prism width [mm]
$\%c_{\text{cutoff}}$	=	percentage cutoff

## I. Introduction

SCHLIEREN imaging is a common flow visualization tool that provides primarily qualitative information related to the refractive index gradient in a transparent medium, which is directly related to the density gradient in gases via the Gladstone-Dale relation. In a conventional schlieren system, either a dual-field-lens or dual-parabolic-mirror Z-type arrangement is used where light is collimated from a point source and passed through a measurement volume, where the variations in refractive index cause small angular deflection to the rays. The second lens or mirror then focuses the rays to a filter, such as a knife edge cutoff, and then a camera is used to image the resulting filtered pattern. Settles provides a history of the development of conventional schlieren in Ref. [1] and a review of more recent developments in schlieren technology in Ref. [2]. Weisberger and Bathel describe the drawbacks of conventional schlieren systems in Ref. [3]

\*Graduate Research Assistant, Mechanical and Aerospace Engineering, 2123 Martin Luther King Jr. Drive, AIAA Student Member.

†Assistant Professor, Mechanical and Aerospace Engineering, 2123 Martin Luther King Jr. Drive, AIAA Senior Member.

which include, but are not limited to, the path integration of non-pertinent flow features in the density structures of interest, limited field-of-view (FOV) from the optical components, a required optical access for clear line of sight, and high-quality surface flatness of the optics.

Focusing schlieren is a variant schlieren imaging technique that allows the user to filter out unwanted features along the line of sight of the system by imaging the density gradients over a plane with narrow depth-of-focus (DOF), instead of full path integration along the collimated beam as in conventional schlieren [4]. Additionally, focusing schlieren does not need high-quality surface flatness windows, as they are out of focus, nor the large focusing mirrors that conventional schlieren requires. However, Bathel and Weisberger point out that the most significant hurdle in deploying focusing schlieren is the alignment procedure, which requires a perfectly matched cutoff grid that is scaled to an image of the source grid. Bathel classifies modern focusing schlieren systems into five types [4]. In each of these, significant effort is required to align the source and cutoff grid elements to one another, and the systems are prone to vibrations.

Recently developed instruments allow for so-called self-aligning systems, where the system projects an image of a physical grid elements onto a background and then re-images the projection back onto the physical grid element [3, 5]. A schematic of such a system is shown in Fig. 1. Polarization is used to separate the outgoing light from the light source, which is polarized with a linear polarizer (LP), from the incoming light to the camera. A quarter wave plate (QWP) is used to convert between linearly and circularly polarized light. By projecting the image of the cutoff grid to a background, the cutoff grid is matched and scaled perfectly to the source grid. The sensitivity of other types of focusing schlieren systems is adjusted by translating the cutoff grid. However, since the system developed by Weisberger and Bathel is self-aligning, this translation will not adjust the sensitivity, and so a Rochon prism (RP) is used to redirect the light returning from the projected grid element such that the image it formed could be translated relative to that grid element. Thus, the Rochon prism can be translated along the optical axis to adjust the sensitivity of the focusing schlieren system. This project will involve such a compact, self-aligning focusing schlieren system whose design is similar to that described in Ref. [3], and shown in 1.

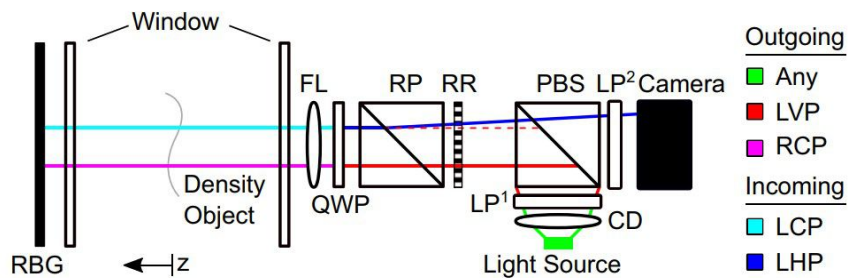


**Fig. 1 Compact, self-aligned, focusing schlieren schematic. The colors represent polarization states of outgoing and incoming light. Credit: NASA [3].**

In a compact focusing schlieren system, light is projected through a Ronchi ruling (RR) onto a retro-reflective background (RBG) where it forms the image of the ruling. The light from this projected image is then reflect back onto the original grid ruling, with a polarizing prism imparting a small offset between the two. The sensitivity of the resulting schlieren can be adjusted by translation of the prism along the instrument axis. The QWP and polarizing beamsplitter (PBS) ensure the returning light from the projected grid element is rotated by  $90^\circ$  relative to the outgoing light. While the system is not overly complex, it can be challenging to design and construct a working system without prior experience. The primary objective of this work is to present both a computational tool which can be used to design a compact, self-aligning focusing schlieren system, and a set of detailed instructions, including troubleshooting, on how to set up and align the system properly.

## II. ATLAS

An aspect that makes constructing a new focusing schlieren system challenging is the fact that it can be difficult to know the requirements for high quality imaging, as it is dependent on the application. In this section, we introduce an assistive design tool called ATLAS (Assistive Tool for seLf-Aligning Schlieren) where the “must-haves” can be entered by the user, and subsequently are used to calculate the specifications of the necessary optics and their positions that will provide for high quality imaging without entirely resorting to a guess-and-check method. Some of the design decisions

the tool assists in determining are:

- Location of the Ronchi ruling, and retroreflective background
- Whether a relay lens is required for the camera
- Focal lengths of the field lens and, if needed, the relay lens
- Rochon prism refraction angle
- Ronchi ruling line pair spacing or frequency
- Determining the space required for the Rochon prism to move relative to the Ronchi ruling to ensure sufficient sensitivity and prevent vignetting
- Approximate field of view and depth of field
- Approximate size of retroreflective background needed
- Total system magnification
- Available distance for translation of the RP along the optical axis
- Minimum and maximum  $\%_{\text{cutoff}}$

ATLAS is a spreadsheet-based calculation tool, which is available as a downloadable Microsoft Excel spreadsheet from our research website at <https://case.edu/engineering/labs/fpi/sites/case.edu/fpi/files/2022-12/ATLAS.xlsx>.

To demonstrate how ATLAS can be utilized in building a new self-aligning focusing schlieren system, we will use the tool as if we were building the system in the Flow Physics and Imaging Lab (FPI) at Case Western Reserve University (CWRU) which can be seen in Fig. 2. A full list of the components is available in Appendix A.



**Fig. 2** Picture of the compact, self-aligning focusing schlieren system in the FPI lab at CWRU.

### III. ATLAS design walkthrough

The design will be built around a fixed location of the field lens and a general schematic can be seen in Fig. 3. The schematic in Fig. 3 shows the outgoing and ingoing polarization states of light, and each optical component. Test windows ( $TW^1$  and  $TW^2$ ) are not necessary, but are shown in the schematic for generality. Our design requires the RR to be close to the FL such that it is too difficult to fit the QWP and RP in between the FL and RR, so the QWP and RP are placed ahead of the FL, between the FL and the RBG. ATLAS currently requires the QWP and RP to be placed after the FL, but the ability to use additional arrangements of these optics in ATLAS, such as those seen in Fig. 1. will be implemented in the future. Additionally, the QWP can be replaced by a quarter-wave film (QWF) placed over the RBG, which removes the spatial sizing limitation of the QWP after the RP. Additionally, the tool will not take the sizes of the

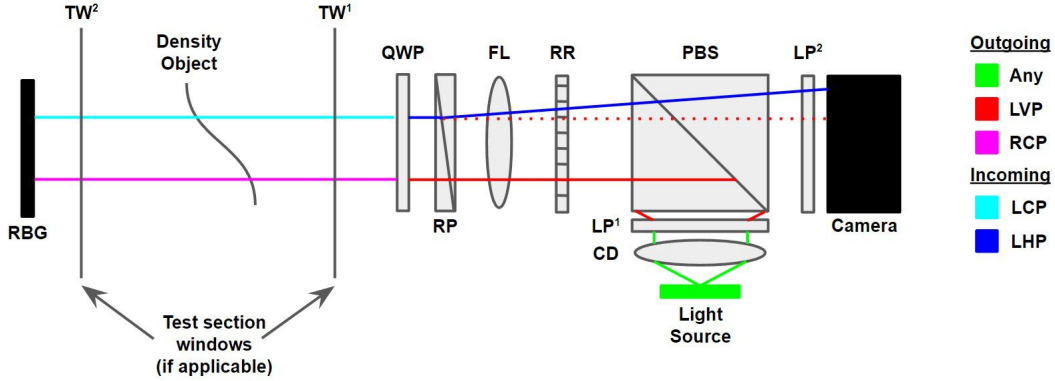


**Fig. 3 Schematic of the compact, self-aligning focusing schlieren system in the FPI lab at CWRU. The colors represent polarization states of outgoing and incoming light.**

PBS, LPs, CD, or QWP into account when determining the other optical locations, or for the calculation of available space for translation along the optical axis of the RP.

**A. Locations of the Ronchi ruling (RR), retroreflective background (RBG), density object (DO), and relay lens (RL)**

Preliminary placement of the optics requires two values: the focal length of the field lens ( $f_{FL}$ ) and the test section width. The test section width for a self-aligning focusing schlieren system of the type in Fig. 3 is approximately the distance between the field lens and the RBG ( $d_{FL-RBG}$ ), plus or minus a small amount for the thicknesses of the optics and windows (if any), and is essentially a choice that is experiment-specific. The focal length of the field lens will determine multiple variables, including the field of view (FOV), which also dependent on the sensor size and the location of the density object. Additionally, the shorter the focal length of the field lens, the brighter the light source will need to be because the light will be spread over a larger area. We strongly recommend using a camera lens, such as a Nikon lens, for the field lens, instead of a single convex or plano-convex lens from a manufacturer such as Thorlabs, as this will remove the need for translating the optic to adjust the focus by simply using the focusing ring on the lens. The system is extremely sensitive to the focal plane of the FL. Figure 4 demonstrates this sensitivity, showing the difference between the focusing ring of the FL being set to the correct position in Fig. 4a and the focusing ring being rotated just  $5^\circ$  past the correct position in Fig. 4b.

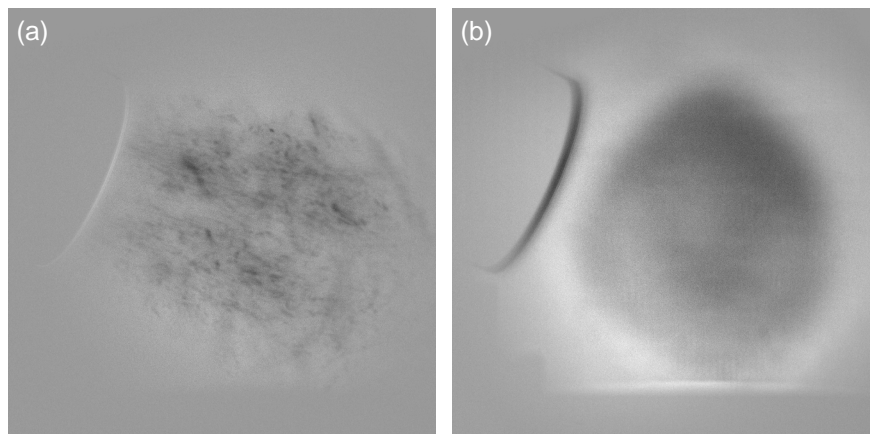


**Fig. 4 Background-subtracted shadowgraph image of a hair dryer jet with focusing ring set to (a) the correct position and (b) the focus ring rotated  $5^\circ$  past the proper position.**

After choosing the location of the RR, RBG, DO, and  $f_{FL}$ , ATLAS will show the diagonal size of the FOV at the density object location to ensure its size is adequate for the desired experiment. For this example, we chose

$d_{\text{FL-RBG}} = 1000$  mm to fit on an available lab table and a Nikon Nikkor 50 mm lens for the field lens. Inputting both of these values into ATLAS returns  $d_{\text{FL-RR}}$  by applying the thin lens equation:

$$\frac{1}{f_{\text{FL}}} \approx \frac{1}{d_{\text{FL-RBG}}} + \frac{1}{d_{\text{FL-RR}}} \quad (1)$$

The calculated value is  $d_{\text{FL-RR}} \approx 52.6$  mm, and so the Ronchi ruling will be preliminarily placed 52.6 mm from the field lens. To check this placement, a light source can be used to project the Ronchi grid onto the RBG. It should appear sharp; a coarse line spacing is useful for this check. An example of what this looks like for the CWRU system with a 1 lp/mm RR can be seen in Fig. 5.

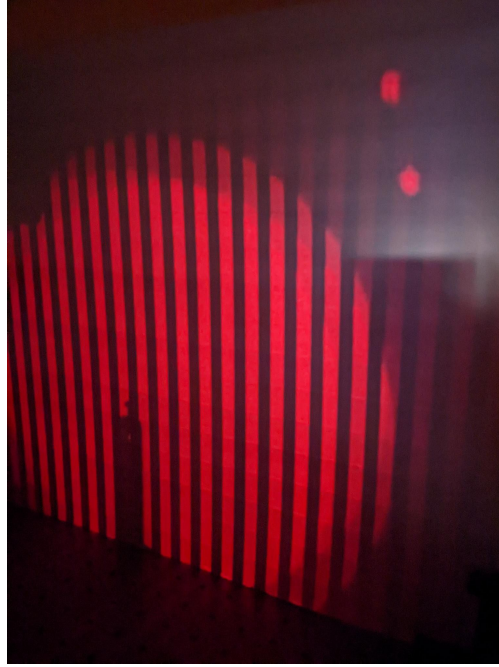


**Fig. 5 RR grid sharply projected onto the RBG.**

Next, the location of the density object relative to the field lens ( $d_{\text{FL-DO}}$ ) is used in the thin lens equation to determine the location of the image relative to the field lens ( $d_{\text{FL-IM}}$ ). In our case, we choose the center of the test section for the DO. Inputting  $d_{\text{FL-DO}} = \frac{1}{2}d_{\text{FL-RBG}} = 500$  mm, ATLAS outputs  $d_{\text{FL-IM}} \approx 55.5$  mm. In this case, ATLAS will also output a warning that a relay lens (RL) may be needed since the image of the density object is only about 3 mm in front of the Ronchi ruling and there is likely not enough room to fit the polarizing beam splitter (PBS) and linear polarizer ( $\text{LP}^2$ ) between the RR and the camera sensor.

If a relay lens is required, then ATLAS is designed to output the distance between the relay lens and the field lens ( $d_{\text{FL-RL}}$ ) by taking the focal length of the relay lens ( $f_{\text{RL}}$ ) and the distance from the camera lens to the camera sensor ( $d_{\text{RL-CAM}}$ ), and solving the thin lens equation for the distance from the relay lens to the image produced by the density object behind the Ronchi ruling ( $d_{\text{RL-IM}}$ ) and adding the distance from the field lens to the image ( $d_{\text{FL-IM}}$ ). These distances are summarized and shown in Fig. 6. Note that the field lens serves two purposes in this type of system. First, it focuses the outgoing light such that an image of the Ronchi ruling is formed on the RBG. Second, it focuses the light reflected off of the RBG such that an image of the density object is formed onto a location behind the Ronchi ruling. This focused image can either be placed directly onto the camera sensor, or if the camera must be positioned further away to accommodate the PBS and  $\text{LP}^2$ , then a relay lens can be used to focus that image onto the camera sensor, as depicted in Fig. 6.

In our setup, we chose a macro lens with 75 mm focal length for the relay lens, and connected it directly to the camera. With this configuration, the distance from the relay lens to the camera,  $d_{\text{RL-CAM}}$  was measured to be 150 mm. Then, using the thin lens equation as previously described, ATLAS outputs  $d_{\text{FL-RL}}$  to be 210 mm. At this point, the RBG, DO, FL, RR, RL, and camera's preliminary locations are determined. These locations assume thin, perfect optics

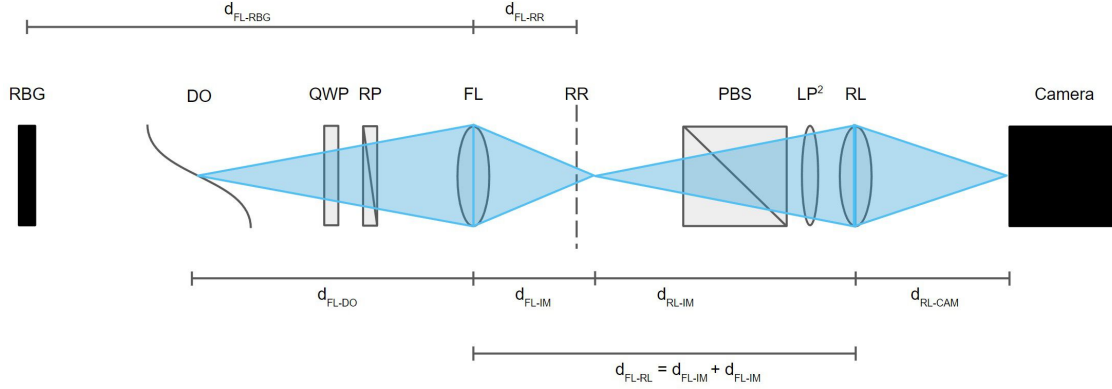


**Fig. 6 Schematic of important distances for preliminary optic placements with a two lens system. Image relay is shown from the density object to the camera sensor.**

so it is possible that slight adjustments are necessary to produce the highest quality schlieren images capable from the system. A simple way to check proper positioning of the optics is to place a screw at the density object location and make sure the camera sharply images the screw threads as seen in Fig. 7.



**Fig. 7 Correctly placed and focused optics sharply imaging a screw.**

### B. Choosing a Rochon prism with suitable cutoff

The next step is to choose a Rochon prism, a schematic of which is seen in Fig .8, for suitable cutoff. Alternatively, focused shadowgraph images can be created by not using a Rochon prism, as shown in Fig. 4a. It is important that the Rochon prism be oriented such that it splits the light along the return path from the RGB, not the outgoing light towards the RGB, and that the axis of separation is parallel to the direction of the lines in the RR.

The cutoff is approximately given by [3]:

$$\delta_{\text{cutoff}} \approx \left( \frac{t_{\text{RP}}}{2} + d_{\text{FL-RP}} \right) \tan(\beta) \quad (2)$$

and the percent cutoff as:

$$\%_{\text{cutoff}} \approx 2\delta_{\text{cutoff}} C_{\text{cutoff}} \quad (3)$$

Since the cutoff is coupled to the parameters of the RP, the line spacing of the RR, and the distance between the RR and the RP, there are likely multiple options that will provide the desired cutoff for a given application. However, since

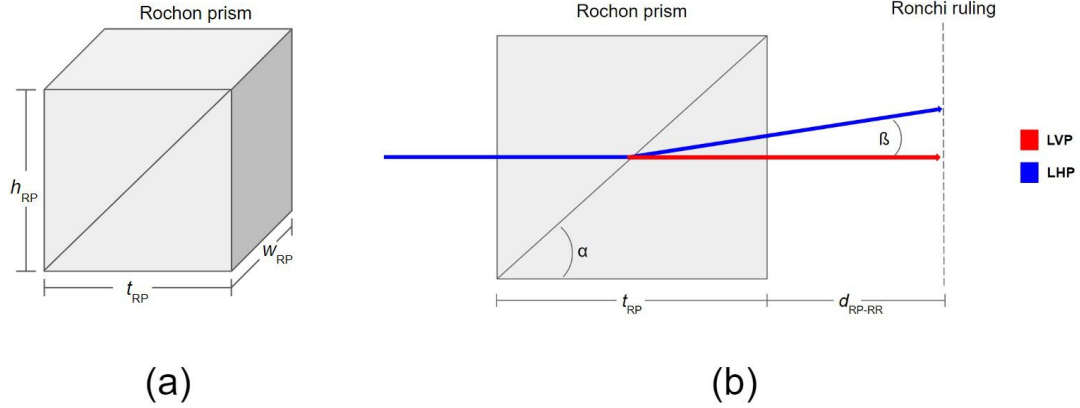


**Fig. 8 Schematic of a Rochon prism showing (a) the overall dimensions and (b) the interface angle ( $\alpha$ ), beam exit angle ( $\beta$ ), thickness ( $t_{RP}$ ), and distance from Rochon prism to Ronchi ruling ( $d_{RP-RR}$ ).**

the RP parameters and line spacing of the RR can be variable, the available distance for RP translation should first be identified. The theoretical maximum of  $d_{RP-RR}$  would be  $d_{RR-DO}$  if the test section does not include windows and vignetting is not a concern, while the minimum of  $d_{RP-RR}$  would be  $d_{FL-RR}$ . In ATLAS, there is a cell to input the  $TW^1$  location and  $d_{FL-RR}$  has already been calculated so the maximum and minimum positions of the RP will be shown.

The next step is to choose the Rochon prism parameters. This should be done somewhat in conjunction with choosing the RR line spacing, found in Sec. III.C, but in our experience Ronchi rulings are cheaper than Rochon prisms and so it is recommended to purchase multiple RR's with line spacings between 1 lp/mm and 40 lp/mm, so there is more flexibility with the Ronchi ruling than with the Rochon prism. When selecting a Rochon prism for purchase, there are a few things to be mindful of:

- The prism dimensions  $h_{RP}$  and  $w_{RP}$  can limit the maximum  $d_{RP-RR}$  if the light from the field lens expands beyond the perimeter of the RP, causing vignetting.
- $t_{RP}$  increases the minimum  $\%_{cutoff}$ .

We initially chose to use a  $75 \times 75$  mm Rochon prism with a thickness of 10 mm from United Crystals with a beam exit angle of  $0.125^\circ$ , but have since purchased a  $0.250^\circ$ ,  $50 \times 50$  mm RP to increase cutoff, downsizing the prism because vignetting will not be an issue. ATLAS allows for inputs of  $t_{RP}$ ,  $h_{RP}$ ,  $w_{RP}$ ,  $\beta$ , and  $d_{RP-RR}$ , and will calculate the  $\delta_{cutoff}$  and  $\%_{cutoff}$  values at the minimum, maximum, and inputted  $d_{RP-RR}$  for a given Ronchi ruling frequency, as well as checking for vignetting issues and showing an error if it might occur. If the size of the RP cannot be increased, but would cause vignetting at max  $d_{RP-RR}$  and there is still a need for more cutoff, then the splitting angle of the prism will need to be increased.

### C. Choosing a Ronchi ruling frequency

For smaller scale systems, the lower line spacings such as 1 lp/mm or 2 lp/mm can work well, while for larger systems higher frequencies such as 5 lp/mm, 10 lp/mm, or 20 lp/mm might be necessary. Additionally, the sharpness adjustment of the projected Ronchi grid onto the RBG during the preliminary optical placements (cf. Sec. III.A and Fig. 5) is much easier with a lower frequency Ronchi ruling. We initially purchased 1 lp/mm, 2 lp/mm, 5 lp/mm, 10 lp/mm, and 20 lp/mm frequencies from Data Optics Inc. to test each in different configurations and have since also purchased 30 lp/mm and 40 lp/mm frequencies. While it may seem obvious to increase the frequency to obtain higher cutoff, there is a trade-off with diffraction issues at higher frequency Ronchi rulings, and so it is difficult to know what will work best for any particular setup. We found that a 20 lp/mm had the best trade-off between diffraction issues and signal. In addition, low frequency rulings tend to be visible in the focusing schlieren images even though the RBG is far from the focal plane of the system, as observed in Fig. 9a. This can be corrected using background subtraction, but it is best to avoid it. During our initial setup, we used the 1 lp/mm RR to assess the sharpness of the projected grid on the RBG but did not change it for a higher frequency RR when attempting to perform schlieren experiments and could not see any flow features. It was not until switching to a higher frequency RR of 5 lp/mm that the density gradients started to become visible. The effect of RR line spacing can be seen in Fig. 9 where the only change made between images is

swapping out the RR.

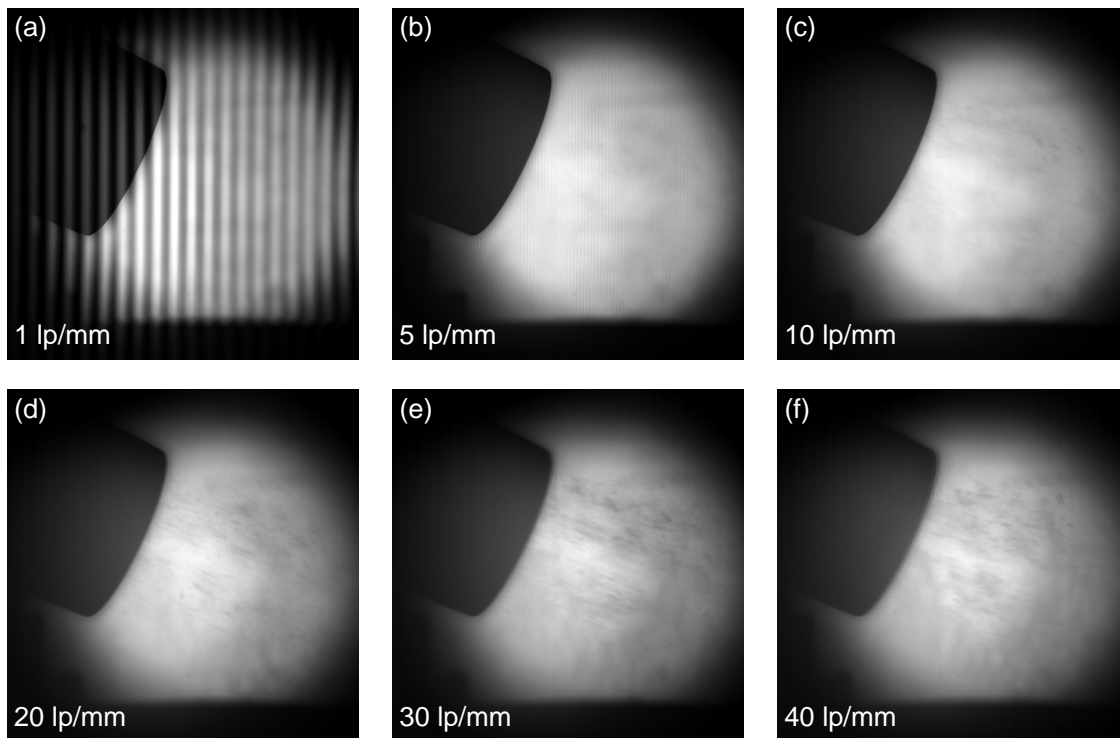


**Fig. 9** Images of non-background subtracted heat gun jet with RR frequency of (a) 1 lp/mm, (b) 5 lp/mm, (c) 10 lp/mm, (d) 20 lp/mm, (e) 30 lp/mm, and (f) 40 lp/mm.

#### D. The retroreflective background

The RBG must do two things: (1) rotate the polarization state from RCP to LCP and (2) reflect the outgoing beam back along the optical axis. In our first RBG, we used strips of reflective tape on poster-board. We found that the soft poster-board material was not a good choice for the tape, since dents or scratches appear in the image if the focal plane is near the RBG. For our system, when  $d_{\text{RBG}}$  was 1000 mm and  $d_{\text{DO}}$  was 600 mm, these imperfections were visible. Additionally, as the focal plane nears the RBG the lines formed by the individual strips of tape become visible in the image, an example of which can be seen in Fig. 12a. While larger strips of tape are available, they can become prohibitively expensive. Coupled with the fact that for large FOV systems the amount of space required for an RBG can become very large, creating a suitable RBG can be exceedingly tedious. In order to address these issues, we have started exploring retroreflective fabrics. While many fabrics can reflect light, one that also rotates the polarization state has proven more difficult to find. However, a material has been found that has both of these properties, an image of which can be seen in Fig. 10.

In Fig. 10a, the RBG has been moved to the right, halfway out of the image so that only about a half circle to the right of the blue dashed line of light is being returned to the camera. In Fig. 10b a piece of the fabric is being held in the area where there is no reflective tape and is denoted by the enclosed yellow dashed line. The reflectance of the fabric is only slightly ( $\sim 10\%$ ) lower than that of the tape, which can be addressed easily by using a more powerful light source. We believe that using this material and pulling it taught, either on a fixed background surface or mounted to a collapsible frame, will provide similar schlieren image quality, but be much easier to build, cheaper to purchase, and more versatile as it will remove the spatial limitations of a rigid background. The fabric shown in Fig. 10 is described by the seller as being 100% polyester, so it is resistant to wrinkles, tears, and other forms of damage.

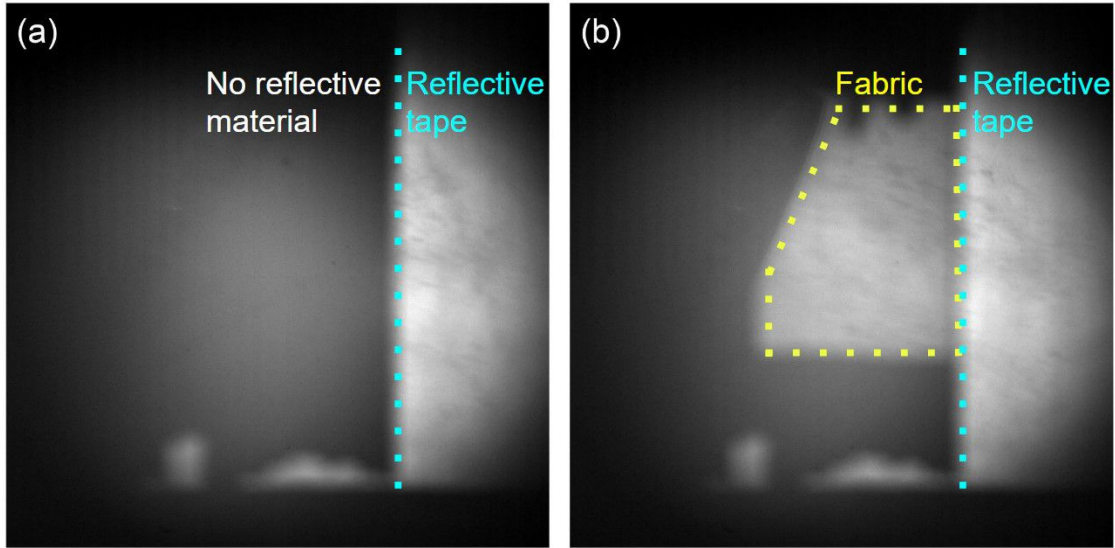


**Fig. 10** Image of heat gun jet with RGB moved halfway out of the FOV to the right with (a) no reflective fabric in the left half and (b) a swatch of reflective fabric being held whose perimeter is indicated by the yellow dashed line.

**E. The polarizing beamsplitter, linear polarizers, condenser/diffuser, and quarter-wave plate or quarter-wave film**

We have only used one PBS, on recommendation that it performed better than another with certain light sources. We cannot therefore provide guidance on how to choose the best PBS for ensuring the highest quality signal at this time, although it is likely that PBS's available from Thorlabs or other similar vendors would perform comparably. The only important factor for the PBS is its size, which should be large enough to accommodate both the outgoing light from the light source and the incoming light to the camera without causing vignetting, and its orientation, which is shown in Fig. 11.

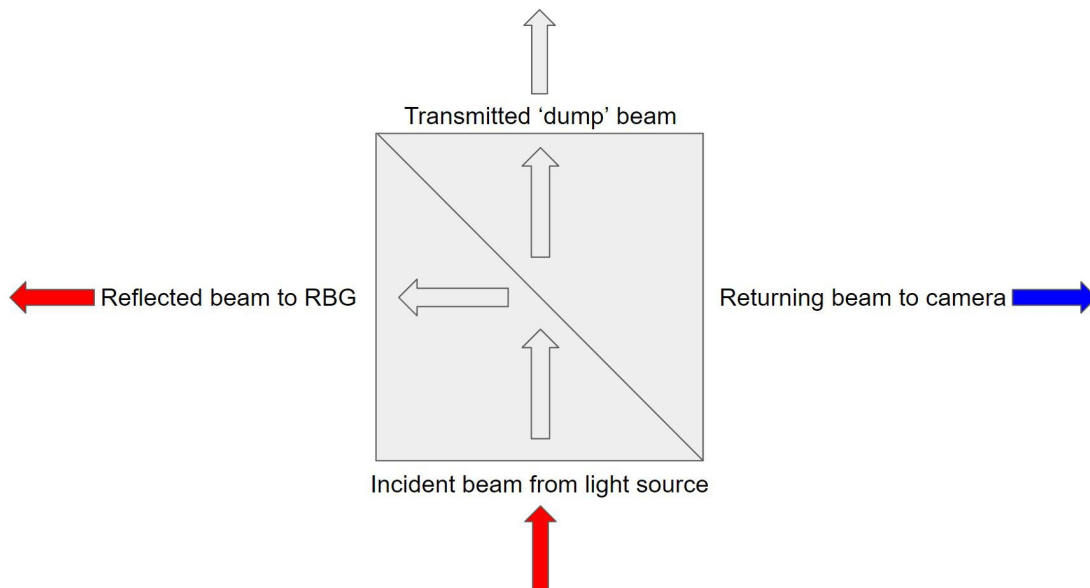


**Fig. 11** Schematic of correctly oriented PBS with incident beam from light source, reflected beam to RGB, transmitted 'dump' beam, and returning beam to camera labelled.

The linear polarizers and condenser/diffuser lens should be appropriately sized for the desired system to not cause vignetting. Depending on the light source, the CD might not be necessary, but we found that it is helpful for brighter

light sources or any light source with multiple LEDs to increase uniformity in the image. Our system uses a set of three red LEDs mounted in a 3-up configuration. The choice of light source is not critical, although the light must be monochromatic to avoid differential chromatic refraction by the RP. Additionally,  $LP^1$  is required to set the polarization state of the light as it travels through the system if the light being emitted from the light source is not already polarized, but  $LP^2$  might not be necessary depending on how well system is enclosed. We found  $LP^2$  useful for rejecting ambient light due to our system not being fully enclosed. If space past the RP and before the DO or  $TW^1$  is extremely limited or vignetting at the QWP is a potential problem, QWF can be a good alternative. Placing a QWF on the RBG will yield the same results as using a QWP, but care must be taken to apply the QWF uniformly to the RBG so as not to cause distortions.

#### IV. Troubleshooting

This section contains a table of problems we experienced while building the system in the FPI Lab at CWRU, which may be commonly encountered by other first-time users. In addition to these issues, Fig. 12 shows some commonly encountered issues when aligning the system for the first time. Figure 12a shows lines of tape on the RBG, which can be visible in the schlieren images if the DO and RBG are close enough together. This can be resolved by using a large continuous sheet of retroreflective material, such as the fabric mentioned in Sec. III.D. Figure 12b illustrates vignetting caused by the QWP being positioned too far away from the other optics in the system. Figure 12c shows the incorrect result of focusing the relay lens on the RR instead of on the image of the density object created by the field lens.

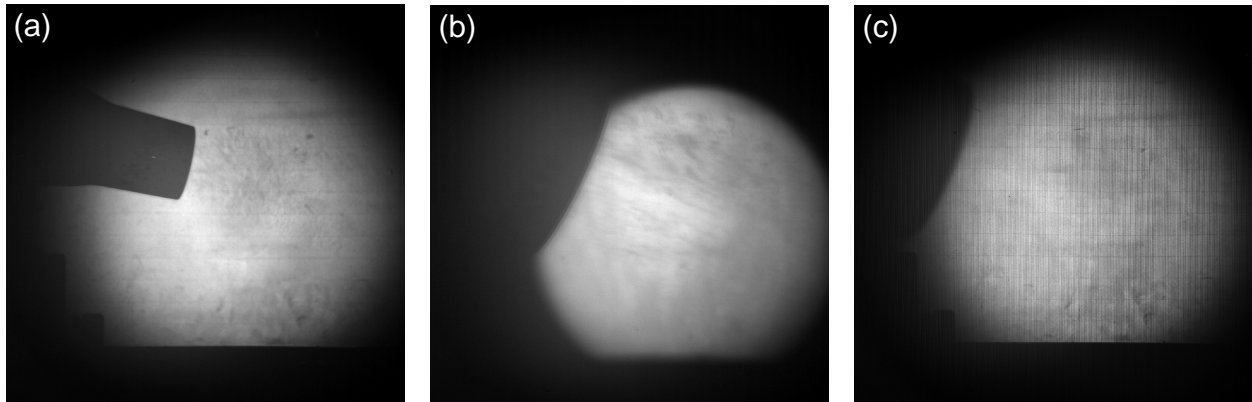


**Fig. 12** (a) Lines of tape visible in the image (b) Strongly vignetted image (c) RL incorrectly focused on the RR instead of on the image of the density object.

Issues	Solutions
We found it difficult to place the optics correctly while using a standard optical lens.	While ATLAS may help with this issue, we bought an F-mount and mounted a Nikon camera lens with focusing ring and strongly recommend this choice.
Once all components of the system were in place and preliminary locations verified using the thin lens equation, we were unable to see flow features.	At the time we were using the 1 lp/mm RR and simply changing to a higher frequency RR fixed this.
We experienced what seemed to be quadrupling of the image in the camera.	Our light source was a triple LED, so each LED was producing its own image in the camera in addition to the final image. Placing a CD after the light source solved this.
When translating the RP, it seemed like the quality of the image did not change.	Our RP was oriented backwards, place it correctly with the exit beam side exiting towards the RR.
It seemed like changes in the field past the PBS did not influence the image. For example, we could block the optical axis entirely and the image would not change.	Our PBS was oriented incorrectly, orient it correctly as described in Sec. III.E.
We observed reflections in the camera images, even with the linear polarizers in place.	Enclose the light source and as much of the system as possible. Make sure if there are any AR-coated optics that the AR-coated side is facing the camera.
Our image seemed to be blurry when using a high frequency RR.	This due to diffraction, and is part of the trade-off in using a higher frequency RR. Lowering the frequency helps, but may also reduce signal quality and/or cutoff.
The camera image was too dark when using a lower focal length field lens for larger FOV's.	Our light source was not bright enough to use a low focal length FL with high FOV.
$d_{RL-CAM}$ was difficult to determine since the RL is encased in lens housing.	Using only the camera and relay lens, we translated a ruler along the optical axis until the image in the camera had a magnification of 1. The relay lens position is then halfway between the ruler and the camera sensor at this magnification.
There were dark spots in the schlieren images that were difficult to remove using post-processing.	These were dents or scratches on the RBG. We re-applied the tape to a rigid surface carefully.

## V. Conclusion

An assistive tool for self-aligning schlieren (ATLAS) has been produced which takes various inputs about the design requirements of the system and assists in the placement and sizing of various optics. A step-by-step walkthrough of building a self-aligning focusing schlieren system of the kind in the FPI lab at CWRU has been presented for first-time users of this type of system. Issues in the initial building and development of the system have been documented with a few associated images to help assist future systems for other builds. Finally, a list of parts in the FPI lab at CWRU is available in Appendix A.

## Acknowledgments

The authors would like to thank Dr. Joshua Weisberger and Dr. Brett Bathel for their assistance in setting up our focusing schlieren system and other helpful conversations. This work was sponsored by the National Institute of Biomedical Imaging and Bioengineering (NIBIB), award no. 1-R21-EB032644-01.

## References

- [1] Settles, G. S., *Schlieren and Shadowgraph Techniques*, 1<sup>st</sup> ed., Springer Berlin Heidelberg, 2001.
- [2] Settles, G. S., and Hargather, M. J., "A review of recent developments in schlieren and shadowgraph techniques," *Measurement Science and Technology*, Vol. 28, 2017. <https://doi.org/10.1088/1361-6501/aa5748>.
- [3] Weisberger, J. M., and Bathel, B. F., "Single source/cutoff grid, self-aligned focusing schlieren system," Vol. 63, 2022. <https://doi.org/10.1007/s00348-022-03389-7>.
- [4] Bathel, B. F., and Weisberger, J. M., "Development of a Self-Aligned Compact Focusing Schlieren System for NASA Test Facilities," , 2022. <https://doi.org/10.2514/6.2022-0560>.
- [5] Bathel, B. F., and Weisberger, J. M., "Compact, self-aligned focusing schlieren system," *Optics Letters*, Vol. 46, No. 14, 2021, p. 3328. <https://doi.org/10.1364/ol.428011>.

## Appendix A

Component	Part#	Supplier
Camera	Nova S12	Photron
Condenser/diffuser	ACL5040U-GD15-A	Thorlabs
Light Source	CREEXPE2-COL-X	LEDsupply
Linear Polarizers	#66-183	Edmund Optics
Optomechanical components	Assorted parts for a 60 mm system	Thorlabs
Polarizing beamsplitter	PBS519	Thorlabs
Retroreflective tape	3M Scotchlite 7610	R.S. Hughes
Rochon prisms	glass/quartz 50 mm x 50 mm, $\beta = 0.125^\circ$ glass/quartz 75 mm x 75 mm, $\beta = 0.250^\circ$	United Crystals
Ronchi rulings	1 lp/mm, 5 lp/mm, 10 lp/mm 20 lp/mm, 30 lp/mm, 40 lp/mm	Data Optics Inc.
Quarter-wave plate	#AQ-200-0545-RET-ACH-L/4	Meadowlark Optics